Proceedings of the Seventeenth (2007) International Offshore and Polar Engineering Conference
Lisbon, Portugal, July 1-6, 2007

ISBN 978-1-880653-68-5; ISBN 1-880653-68-0(Set); ISSN 1098-6189 (Set)

Probabilistically-robust nonlinear control of offshore structures

Alexandros A. Taflanidis [1], *Demos C. Angelides* [2] *and James L. Beck* [1]

[1] Division of Engineering and Applied Science, CALTECH
Pasadena, California, USA.

[2] Department of Civil Engineering, Aristotle University of Thessaloniki
Thessaloniki, Greece

ABSTRACT

A controller design for offshore structures is discussed in this study. Stochastic simulation is considered for evaluation of the system's performance in the *design stage*. This way, nonlinear characteristics of the structural response and excitation are *explicitly* incorporated into the model assumed for the system. Model parameters that have some level of uncertainty are probabilistically described. In this context, the controller is designed for optimal reliability, quantified as the probability, based on the available information, that the performance will not exceed some acceptable bounds. This treatment leads to a robust-to-uncertainty design. The methodology is illustrated in an example involving the control of a Tension Leg Platform in a random sea environment. Multifold nonlinearities are taken into account for the evaluation of the platform's dynamic response and a probabilistic description is adopted for characterizing the random sea environment.

KEY WORDS: Control of offshore structures; Tension Leg Platform; robust control; model uncertainty; stochastic simulation; random sea.

INTRODUCTION

Under severe sea and wind conditions, offshore structures, such as jacket-type or tension leg platforms, may experience large response amplitudes that affect their serviceability and structural integrity. Active and passive control techniques have been considered for reduction of the effects of such dynamic loadings (Ahmad and Ahmad, 1999; Alves and Batista, 1999; Nakamura, Kajiwara, Koterayama and Hyakudome, 1997; Suhardjo and Kareem, 2001). Most of the studies in offshore structure control have adopted linear methodologies for the controller design, typically H_2 control. The models, though, that are used for the prediction of the behavior of offshore structures typically involve various types of nonlinearities. In particular, nonlinearities may come from (a) modeling the dynamic response of the structure (for example, in the case of Tension Leg Platforms, as discussed in Angelides, Chen and Will (1982)) and also from (b) characterizing the excitation forces acting on the structure (for example, the spectrum for random sea environment or the wave particle kinematics (Goda, 2000)). One of the main challenges in controller design for offshore applications has been the explicit consideration of these nonlinearities.

Enhanced linearization techniques have been suggested for addressing the second type of nonlinearity when applying linear control methodologies (Suhardjo and Kareem, 2001). This approach has the potential to adequately capture important nonlinear characteristics of the response; but for complex systems the application is usually not straightforward. The first type of nonlinearity, which is more important, is commonly ignored. The controlled system is usually designed based on a linear model, that does not take into account nonlinear characteristics (Ahmad and Ahmad, 1999; Alves and Batista, 1999). Only the performance of the system is evaluated using, at a later stage, a nonlinear model (Ahmad and Ahmad, 1999). This approach leads to a sub-optimal design in terms of the actual system performance.

Another challenge related to offshore structure control has been the efficient description of the uncertainties involved in the system model. In maritime applications, like most other engineering applications, there are model properties that involve some level of uncertainty (for example the characteristics of the sea environment). This uncertainty can be quantified by a probabilistic description of the model parameters (Mathisen and Bitner-Gregersen, 1990; Papadimitriou, Beck and Katafygiotis, 2001). Such an approach logically incorporates the available knowledge about the system into the model and allows for a robust-to-uncertainty design. Typically, though, a nominal model is adopted when designing the controlled system, using the most probable values for the model parameters. No uncertainty for these values is taken into account.

The current study considers a controller design for offshore applications that addresses both aforementioned challenges. Simulation is used for evaluation of the model response at the controller design stage, which allows for *explicitly* taking into account nonlinear characteristics of the system. Uncertainty about the model parameters is treated by assigning probability density functions (PDFs) to them. In this context, reliability criteria are used to evaluate the performance of the controlled system and for the controller optimization. An efficient algorithm is discussed for the latter. The methodology is illustrated in an example involving the control of a Tension Leg Platform in a random sea environment. The control force is provided by tuned mass dampers, placed inside the columns of the platform's hull. Both passive

and active applications are discussed. A realistic setting is considered for the latter; actuator saturation, availability of only noisy acceleration measurements, and time delays in the control loop are assumed. Multiple nonlinearities are taken into account for the platform's response and probabilistic description is adopted for the system model.

ROBUST NONLINEAR CONTROLLER DESIGN USING STOCHASTIC SIMULATION

System model

Consider a controlled system under stochastic excitation (Fig.1):

$$\begin{aligned}\dot{\mathbf{x}}(t) &= \mathbf{F}(\mathbf{x}(t),\mathbf{u}_c(t),\mathbf{q}(t))\\ \mathbf{y}(t) &= \mathbf{J}(\dot{\mathbf{x}}(t),\mathbf{x}(t),\mathbf{u}_c(t),\mathbf{q}(t)) + \mathbf{n}(t)\\ \mathbf{z}(t) &= \mathbf{H}(\dot{\mathbf{x}}(t),\mathbf{x}(t),\mathbf{u}_c(t),\mathbf{q}(t))\end{aligned} \quad (1)$$

where $\mathbf{x}(t)$ is the system state vector, composed of the structural states together with any ancillary states used to model sensor and actuator dynamics, $\mathbf{y}(t)$ is the measurement vector, $\mathbf{z}(t)$ is the predicted output vector, $\mathbf{u}_c(t)$ is the control input, $\mathbf{n}(t)$ is the measurement noise and $\mathbf{q}(t)$ is the stochastic excitation vector. The performance of the controlled system is assessed through the favorability of output vector $\mathbf{z}$ composed of response quantities (performance variables) that are considered important for the system design, such as maximum displacements, accelerations or member strain. The control input is designated as a potentially nonlinear, feedback function of the measurement vector:

$$\mathbf{u}_c(t) = \mathbf{K}(\mathbf{y}(t)) \quad (2)$$

This formulation covers both passive and active (or semi-active) control implementations. For systems with passive control devices (i.e., viscous dampers and springs), the "feedback" measurements $\mathbf{y}$ consists of relative velocities (for dampers) and relative displacements (for springs), no measurement noise is considered and $\mathbf{K}$ is composed of the viscosity (for the dampers) or the stiffness (for the springs) parameters.

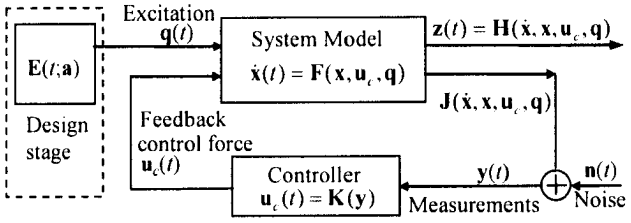

Fig.1 : Schematic of the model for the controlled dynamical system.

For offshore structures, the excitation vector $\mathbf{q}(t)$ typically includes the characteristics for the environments of wind (velocity profile) and sea (free surface elevation and water particle velocities and accelerations). When evaluating the controlled system performance, $\mathbf{q}(t)$ may be described by time-histories of actual excitation records. In the controller design stage, the excitation is predicted by the model:

$$\mathbf{q}(t) = \mathbf{E}(t;\mathbf{a}) \quad (3)$$

where $\mathbf{a}$ is the vector of model parameters. This formulation allows for directly considering known characteristics of the excitation (for example, spectral properties) at the design stage. The controller, $\mathbf{K}$, is optimized taking into account all available information for the system and its loading conditions, which can lead to a significant improvement in performance.

Probabilistic model uncertainty and reliability framework

Since the knowledge about a system in engineering applications is never complete, the concept of reliability has been incorporated into engineering design as a means of explicitly taking into account model uncertainties. In this context, assume that the properties of the models (1) or (2) depend on a set of h uncertain parameters and let the vector of these parameters be $\boldsymbol{\theta} \in \Theta$, where $\Theta \subset \mathbb{R}^h$ denotes the set of possible parameter values. The available knowledge about the values of these parameters is incorporated into the model by assigning a PDF, $p(\boldsymbol{\theta})$, to them. The existence of non-parametric, unmodeled, uncertainty may be addressed by introducing a model prediction error ε, i.e. an error between the response of the actual system and the response of the model adopted for it (Papadimitriou, Beck and Katafygiotis, 2001).

The reliability of the system is quantified by a measure of the plausibility of system "failure", based on the available information. "Failure", here, is interpreted as any performance variable exceeding acceptable bounds, or equivalently that the response vector of the system, $\mathbf{z}(t)$, will exit a safe domain D_s within the duration of the excitation $t \in [0,T_t]$. Let $g(\boldsymbol{\theta},\mathbf{K})>0$ be the limit state function defining the *model's* failure. If $\mathbf{z}=[z_1 \ldots z_n]$, D_s and $g(\boldsymbol{\theta},\mathbf{K})$ are defined as:

$$D_s = \bigcap_{i=1}^{n} \{z_i \le \beta_i\}, \quad g(\boldsymbol{\theta},\mathbf{K}) = \max_{t,i}\left(z_i(t)/\beta_i(t)\right) - 1 \quad (4)$$

where β_i corresponds to the acceptable threshold for the i^{th} performance variable. If $g_a(\mathbf{K})$ is the quantity defining the actual system's failure, then the model prediction error is defined as $\varepsilon(\boldsymbol{\theta},\mathbf{K})=g_a(\mathbf{K})-g(\boldsymbol{\theta},\mathbf{K})$ and may be treated as a random variable with some known distribution (chosen based on observations of the system and model responses). The probability of failure for a given $\mathbf{K}$ is finally expressed as:

$$P(F \mid \mathbf{K}) = P\left(\mathbf{z}(t) \notin D_s \text{ for some } t \in [0,T_t]\right) = \int_{\Theta} I_F(\boldsymbol{\theta},\mathbf{K})\, p(\boldsymbol{\theta}) d\boldsymbol{\theta} \quad (5)$$

where $I_F(.)$, the indicator function for failure, is one if the system fails, i.e $g_a(\mathbf{K})>0$, and zero if not and thus it expresses a binary distinction for the system performance. When a model prediction error is assumed then $I_F(.)$ in (5) can be replaced by $P_\varepsilon(g(\boldsymbol{\theta},\mathbf{K}))$, where $P_\varepsilon(.)$ is the conditional on $\{\boldsymbol{\theta},\mathbf{K}\}$ cumulative distribution function for ε (Taflanidis and Beck, 2007). In this formulation, the influence of the prediction error can be equivalently considered as introduction of a function that incorporates a preference for the system performance (instead of the binary distinction of failure), expressed through the value $P_\varepsilon(g(\boldsymbol{\theta},\mathbf{K}))$.

Another possible quantification of the performance, in this probabilistic setting, would be to use the expected value of the response $E_\Theta[\mathbf{z}]$, where the expectation is expressed over the uncertain parameter space. For engineering applications the reliability formulation provides a more reasonable measure, since most systems perform unacceptably only if the response exceeds some threshold level. It stands to reason then to design a system in order to regulate the response that exceeds these thresholds (as reliability-based design does), rather than focus on the average response. In many applications, of course, these design goals lead to comparable designs, i.e. optimization of the reliability coincides with optimization of the average performance.

Reliability-based design using stochastic simulation

The motivation for the application of control technology to civil engineering systems and the metrics by which the quality of such systems are judged ultimately stems from the concept of system reliability (May and Beck, 1998; Taflanidis, Scruggs and Beck, 2006).

Let K denote the admissible design space for the controller parameters. Then the controller design is to determine $\mathbf{K}$ for optimal reliability:

$$\mathbf{K}^* = \arg\min_{\mathbf{K}\in K} P(F \mid \mathbf{K}) \tag{6}$$

For performing optimization (6), the integral (5) needs to be evaluated. This integral can rarely be calculated analytically, especially for complex systems, and so it is usually estimated by stochastic simulation using a finite number N of random samples of $\boldsymbol{\theta}$, drawn from $p(\boldsymbol{\theta})$. The failure probability and the optimal reliability controller are then:

$$\hat{P}(F \mid \mathbf{K}) = \frac{1}{N}\sum_{i=1}^{N} I_F(\boldsymbol{\theta}_i, \mathbf{K}), \quad \mathbf{K}^* = \arg\min_{\mathbf{K}\in K} \hat{P}(F \mid \mathbf{K}) \tag{7}$$

In this context, the model response, i.e. $g(\boldsymbol{\theta},\mathbf{K})$, can be evaluated through simulation - rather than approximated, for example, analytically as in Taflanidis, Scruggs and Beck (2006). Thus, nonlinearities of the system can be easily incorporated into its model.

The optimization in (7), though, is quite challenging. First of all, the evaluation for $P(F|\mathbf{K})$ involves an unavoidable estimation error since stochastic simulation is used; the existence of this error contrasts with classical deterministic optimization where it is assumed that one has perfect information. Furthermore, each evaluation of the objective function in (7) typically requires a substantial computational effort. The highly efficient Stochastic Subset Optimization (SSO) (Taflanidis and Beck, 2007) may be used to perform optimization (7). The basic idea in SSO is the formulation of an augmented reliability problem, where the controller parameters $\mathbf{K}$ are artificially considered as uncertain with uniform PDF over its set of values K. Stochastic simulation techniques are then used in order to simulate samples of them that lead to system failure. The information that these samples contain is utilized in order to identify regions containing the optimal controller parameters and to iteratively converge to the optimal solution. A single reliability analysis is used at each iteration, which significantly reduces the computational cost. More details are avoided here due to space limitations.

Using SSO, optimization (7) can be efficiently performed; the methodology described in this section corresponds, ultimately, to a robust-to-uncertainty nonlinear design that takes into account all available information and important characteristics (linear or nonlinear) of the system. The only constraint in the complexity of the system description stems from the accessible computational power, since a large number of simulations of the system response is needed. The constant advances in computer technology (hardware and software related) are continuously reducing the significance of this constraint.

This methodology is illustrated next using an application on a Tension Leg Platform (TLP).

MODEL FOR TLP IN RANDOM SEA

TLPs (Fig. 2) are floating structures of semi-submersible type, moored by vertical tendons under initial pretension, T_o, imposed by excess buoyancy. Several TLPs have been used for oil exploration and drilling operations in deep waters. They can be modeled as a rigid body having six degree of freedom, which includes three translations (surge, x, sway, y, and heave, z) and three rotations (roll, φ, pitch, θ, and yaw, ψ). The natural period in surge, sway and yaw are in the range 80-120 sec and well above the range of dominant waves, which typically have periods 6-18 sec. On the other hand the heave, pitch and roll periods are in the range 2-4 sec and below the period of the exciting waves. Thus, forces at the dominant wave frequencies do not excite the TLP at its natural frequencies. Still, higher-order nonlinear forces at the sum and difference of the wave frequencies can produce significant resonant excitations at the TLP natural frequencies because of the small amount of damping available at these frequencies (Mekha, Johnson and Roesset, 1996). Passive and active control techniques have been investigated for reducing the effects of these excitations (Ahmad and Ahmad, 1999; Alves and Batista, 1999).

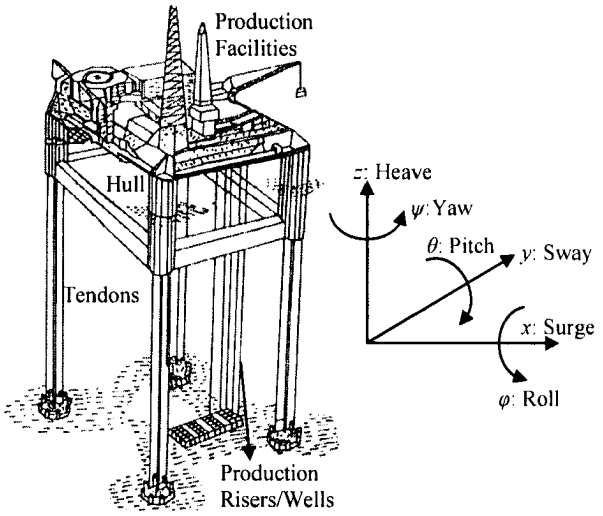

Fig.2 : Tension Leg Platform and degrees of freedom.

In this study, we assume that the direction of wave propagation coincides with one of the axes of symmetry of the platform (Fig. 3). Thus, only 3 degrees of freedom are excited (surge, heave, pitch). Additionally, wave diffraction effects are neglected. Structural damping is also neglected because it can be considered small compared to the hydrodynamic damping (Mekha, Johnson and Roesset, 1996) and the damping provided by the control application.

Various types of nonlinearities are present in the analysis of a TLP (Zeng, Liu, Shen and Wu, 2006). The influence of the change in the submerged TLP surface because of the wave passage and the coupling between the different degrees of freedom in evaluating the tendon stiffness are two of the more important ones. The TLP model assumed here incorporates the most important nonlinearities. The formulation follows closely the one presented in Angelides, Chen and Will (1982) which considers large translations and large rotations for the TLP response. The main characteristics are briefly summarized next.

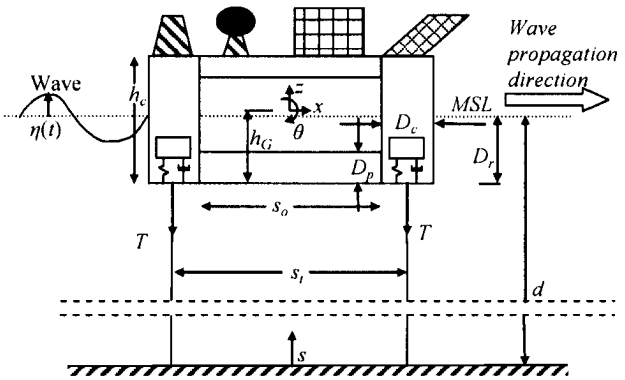

Fig.3 : Tension Leg Platform model considered in this study.

Hydrodynamic and hydrostatic Forces

The hydrodynamic force of the submerged TLP portion is calculated using the Morison equation. For a cylinder with diameter D, the force in the normal direction, per unit length dl, is given by:

$$df(t) = \frac{1}{2}\rho_w D C_D \left(\dot{U}_{wn} - \dot{U}_{sn}\right)\left|\dot{U}_{wn} - \dot{U}_{sn}\right| dl + \frac{1}{4}\rho_w \pi D^2 C_M \ddot{U}_{wn} dl - \frac{1}{4}\rho_w \pi D^2 \left(C_M - 1\right)\ddot{U}_{sn} dl \tag{8}$$

where ρ_w is the density of the sea water, $\ddot{U}_{wn}$ and $\dot{U}_{wn}$ are the wave particle acceleration and velocity normal to the cylinder, $\ddot{U}_{sn}$ and $\dot{U}_{sn}$ are the structural element normal acceleration and velocity, C_D is the drag coefficient and C_M is the inertia coefficient. Both coefficients are assumed here to be same for columns and pontoons, constant along the water depth and frequency independent. The last term in (8) is referred to as the added-mass. For evaluation of the total hydrodynamic forces, the total length of the structural elements (columns and pontoons) is divided into equal length segments. The structural and wave kinematics are then calculated at the centroid of each segment. Based on these values, the hydrodynamic forces are calculated and then multiplied by the segment length to yield the forces at the center of the segment. These forces are then transferred to the center of gravity of the hull to obtain the resultant forces and moments. For the TLP columns the instantaneous submerged depth, accounting for wave passage and structural motion, is considered in the evaluation of the hydrodynamic forces. In addition, the hydrostatic pressures acting on the submerged part of the TLP geometry are integrated at each time instant up to the instantaneous free surface sea level to yield a vertical buoyancy force and moment at the center of gravity of the TLP.

Tendon restoring forces

The tendon stiffness is derived with reference to the instantaneous position of the platform, i.e. displacements in all degrees of freedom are simultaneously considered. The tension on each tendon is:

$$T = \frac{EA}{L}\Delta L + T_o \tag{9}$$

where E is Young's modulus, A the cross sectional area of the tendon, L is the initial length of the tendon and ΔL is the instantaneous change in length. This force is applied along the instantaneous axial direction of the tendon and transformed into the center of gravity of the hull to obtain resultant forces and moments. This formulation introduces a nonlinear coupling between the different degrees of freedom.

Random sea model

Water particle kinematics are modeled according to Airy wave theory. The random sea is modeled as Gaussian process following a modified Pierson-Moskowitz (PM) type spectrum for the free-surface elevation (Goda, 2000):

$$S(\omega) = \frac{H_s^2 T_z}{8\pi^2}\left(T_z\frac{\omega}{2\pi}\right)^{-5}\exp\left[\frac{1}{\pi}\left(T_z\frac{\omega}{2\pi}\right)^{-4}\right] \tag{10}$$

where ω is the frequency, H_s the significant wave height and T_z the zero up-crossing period. To implement this spectrum, the free-surface wave elevation is represented in the time domain by a superposition of a large number of harmonic waves corresponding to different frequencies ω_i:

$$\eta(t) = \sum_{i=1}^{k} A_i \cos(\kappa_i x - \omega_i t + \varphi_i) \tag{11}$$

$$A_i = \sqrt{\left(\alpha_i^2 + \delta_i^2\right) S(\omega_i)\Delta\omega_i}\,,\ \varphi_i = \operatorname{atan}\left(\delta_i / \alpha_i\right) \tag{12}$$

where α_i and δ_i are standard Gaussian variables and $\Delta\omega_i$ is the bandwidth that each harmonic represents. The number of component waves, k, in (11) is a compromise between realizing the Gaussian distribution for the surface elevation and establishing computational efficiency for the simulation of the model response. For determining the sequence $\{\omega_i\}$, the frequency range of interest is divided into sub-ranges and ω_i is chosen as the middle of each one. The bandwidth $\Delta\omega_i$ equals to the width of the respective sub-range. A detailed discussion for determination of these sub-ranges is provided in Appendix A. In (11), κ_i is the wave number, related to the frequency and the water depth, d, through the well known dispersion relationship:

$$\omega_i^2 = g\kappa_i \tanh(\kappa_i d) \tag{13}$$

The water particle kinematics are computed according to Airy linear wave theory with the modification discussed by Chakrabarti (1971) in order to incorporate the effect of variable free surface sea level. The velocity of the water particles in the horizontal and vertical direction is given respectively by:

$$\dot{u}(t) = \sum_{i=1}^{k} A\omega_i \cos(\kappa_i x(t) - \omega_i t + \varphi_i)\frac{\cosh\left(\kappa_i s(t)\right)}{\sinh\left(\kappa_i\left(d + \eta(t)\right)\right)} \tag{14}$$

$$\dot{v}(t) = \sum_{i=1}^{k} A\omega_i \cos(\kappa_i x(t) - \omega_i t + \varphi_i)\frac{\sinh\left(\kappa_i s(t)\right)}{\sinh\left(\kappa_i\left(d + \eta(t)\right)\right)} \tag{15}$$

where $s(t)$ and $x(t)$ are the vertical and horizontal distance, respectively, at which the wave kinematics are evaluated (see Fig. 3). The acceleration may be obtained by differentiation of these relationships.

This model fully characterizes the excitation vector, as in (3). The model parameters are represented by the vector $\mathbf{a}=[H_s, T_z, \{\alpha_i\}, \{\delta_i\}, \{\omega_i\}]$. The excitation vector $\mathbf{q}(t)$ is composed of the free surface elevation and the orthogonal components (horizontal and vertical) of wave particles velocity and acceleration. The latter quantities are resolved to give $\dot{U}_{wn}$ and $\ddot{U}_{wn}$ in (8) according to the instantaneous rotation of the TLP. The free surface elevation is used for estimation of the submerged portion of the TLP hull.

CONTROL IMPLEMENTATION FOR TLP

Various devices have been proposed for control of offshore structures (for example, passive or active tuned mass dampers (TMD), active thrusters, active tendons and pneumatic actuators) depending on the application characteristics (for example, properties of the motion that is controlled). For TLPs, of particular interest is the control of the coupled heave/pitch motion since large displacements in the vertical direction may lead to unacceptable strain for both pre-stressed tendons and production risers. This can be established by TMDs placed in all columns of the hull as suggested in Alves and Batista (1999) and illustrated in Fig. 3. Both passive and active application of TMDs is considered in this study. A simplified schematic is given in Fig. 4. We assume that the TMD's are allowed to vibrate in the vertical only direction. This control implementation allows for directly controlling the heave and pitch response of the structure. The surge response may only indirectly be influenced (through the coupling with the other two degrees of freedom).

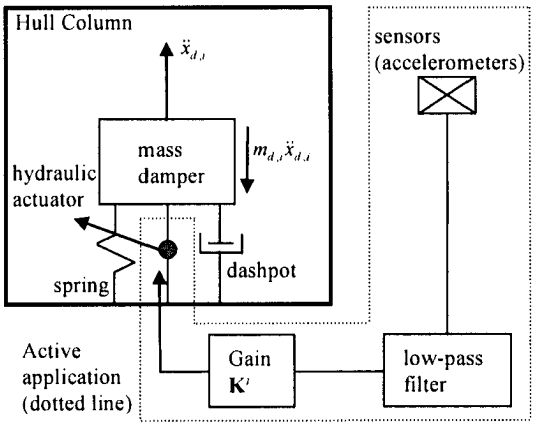

Fig.4 : Schematic of passive and active TMD implementation.

Passive TMD

A TMD consists of a mass attached to the primary structure through a spring and a dashpot. The motion of this mass counteracts against the motion of the platform, thereby providing energy dissipation (inertia force of the damper acting on the structure). The controller parameters **K** in this case consist of the spring and dashpot coefficient or, equivalently, the frequency $\omega_{d,i}$ and the damping ratio $\zeta_{d,i}$ for each damper i, assuming that the mass $m_{d,i}$ of the damper has been already selected (based on consideration about the maximum feasible or allowable additional mass). Excessive vibrations of the TMD can be prevented (due to space limitations) by appropriately placed stoppers.

Active TMD

The effectiveness of TMDs can be enhanced by application of active control forces through hydraulic actuators (Fig. 4). In this study, only noisy acceleration measurements are assumed to be available for the active control implementation. Because of the nonlinear characteristics and the complexity of the system model, estimating its states (velocities and displacements) based on the acceleration measurements cannot be performed accurately (Anderson and Moore, 2005) and is avoided here. Also, because of the presence of noise, double integration of the accelerations to obtain displacement measurements might be unstable and unreliable. Velocity or acceleration feedback are practically the only feasible choices for feedback control design. The latter is selected here and the control force on each damper, u_i, is designated as feedback function of the heave and pitch filtered accelerations; the acceleration measurements are filtered by a low-pass filter in order to reduce the influence of the noise in the signal (Chu, Soong and Reinhorn, 2006). The transfer function of the filter is:

$$H_f(s) = \frac{\omega_f^2}{s^2 + 2\zeta_f \omega_f s + \omega_f^2} \tag{16}$$

where $\zeta_f = \sqrt{2}/2$ and ω_f should be selected higher than the natural frequencies of the system. If $\ddot{z}_f$ and $\ddot{\theta}_f$ are the filtered accelerations, $\mathbf{K}'$ the feedback gain for the i^{th} damper and K_k' its k^{th} element, then

$$u_i = \mathbf{K}'\begin{bmatrix} \ddot{x}_f & \ddot{\theta}_f \end{bmatrix}^T = \begin{bmatrix} K_1' & K_2' \end{bmatrix}\begin{bmatrix} \ddot{x}_f & \ddot{\theta}_f \end{bmatrix}^T \tag{17}$$

Equation of motion for controlled system

The model for the dynamic response of the controlled system is finally:

$$\begin{aligned} m\ddot{x} + F_{r,x} &= F_{d,x} \\ m\ddot{z} + F_{r,z} &= F_{d,z} + F_h - w - \sum_{i=1}^{4} m_d \ddot{x}_{d,i} \\ I_\theta \ddot{\theta} + F_{r,\theta} &= F_{d,\theta} + M_h + \sum_{i=1}^{4} l_i m_d \ddot{x}_{d,i} \\ m_{d,i}\left(\ddot{x}_{d,i} + \ddot{z} - l_i\ddot{\theta}\right) + 2\omega_{d,i}\zeta_{d,i} m_{d,i}\dot{x}_{d,i} + \omega_{d,i}^2 m_{d,i} x_{d,i} &= u_i \quad i=1,\ldots,4 \end{aligned} \tag{18}$$

where $x_{d,i}$ is the relative displacement of the i^{th} mass damper, m is the total mass of the platform (including the TMDs), I_θ is the mass moment of inertia at the center of gravity of the hull (again including the TMDs), $F_{r,j}$ is the resultant restoring force (or moment in the center of mass of the hull) generated by the tendon system in degree of freedom j (j=x,y,θ), $F_{d,j}$ is the similar quantity for the hydrodynamic forces, w is the weight of the structure, F_b is the buoyancy force, M_b is the moment created by that force (again calculated at the center of mass of the TLP) and l_i is the instantaneous horizontal position of damper i with respect to the center of gravity of the hull. In (18), the coupling between the TMD motion and the rotation of the platform is directly taken into account. This coupling was neglected in previous investigations (Alves and Batista, 1999).

CONTROLLER DESIGN AND EVALUATION

The characteristics of the platform considered in this study are shown in Table 1. The natural frequencies of the platform are: heave 3.16sec, pitch 3.13 sec and surge 117 sec. Four mass dampers with individual mass equal to 0.5% of the hull mass are considered, one on each hull column. When considering the total apparent mass of the platform (structural mass+added mass up to mean sea level), this ratio drops to 0.3%. For the active control application, the actuators are modeled as ideal forcing systems (no dynamics) with maximum force capability of 500kN (saturation of actuator forces). Time delay equal to 5ms is also assumed in the control loop. The maximum allowable displacement for the damper is set to 2m and ω_f in (16) is equal to 8rad/sec.

Table 1. Details of TLP.

Column diameter (D_c)	18m	Pontoon diameter (D_p)	12m
Mass	40500 ton	Radius of gyration (pitching motion)	39m
Total pre-tension (T_o)	165 10^3 kN	Structural damping	0%
E of tendons	200 kN/cm^2	Tendon diameter	0.3m
Water depth	640m	Draft (D_r)	33.5m
C_D	1	C_M	2
Distance between columns (s_o)	77m	Column height (h_c)	75m
Position of center of mass (h_G)	38m above keel	Tendons per leg	3

Model Uncertainty

The biggest sources of uncertainty in the TLP and excitation models are the characteristics of the PM spectrum, H_s and T_z. The joint distribution of H_s and T_z has been discussed in numerous studies (for example, in Mathisen and Bitner-Gregersen (1990)) and a variety of statistical descriptions have been suggested. In this study, we adopt a three parameter marginal Weibull distribution for H_s:

$$p(H_s) = \frac{\beta_w}{\alpha_w}\left(\frac{H_s - \gamma_w}{\alpha_w}\right)^{\beta_w - 1} \exp\left(-\left(\frac{H_s - \gamma_w}{\alpha_w}\right)^{\beta_w}\right) \tag{19}$$

and a conditional log-normal for the zero up-crossing period, T_z. The parameters selected for the Weibull distribution are α_w=1.41, β_w=1.2 and γ_w=1, whereas the median, e^{μ}, and logarithmic standard deviation, σ, for the log-normal are (Mathisen and Bitner-Gregersen, 1990):

$$\exp(\mu) = \exp(a_1 + a_2 H_s^{a_3}),\ \sigma = b_1 + b_2 \exp(b_3 H_s) \quad (20)$$

where a_1=1.22, a_2=0.32, a_3=0.52, b_1=0.075, b_2=0.04 and b_3=-0.6. Fig. 5(a) shows the PM spectrum for various H_s and Fig. 5(b) shows a sample realization of the free surface elevation for H_s=9m. In these figures, T_z is set to its conditional mean value.

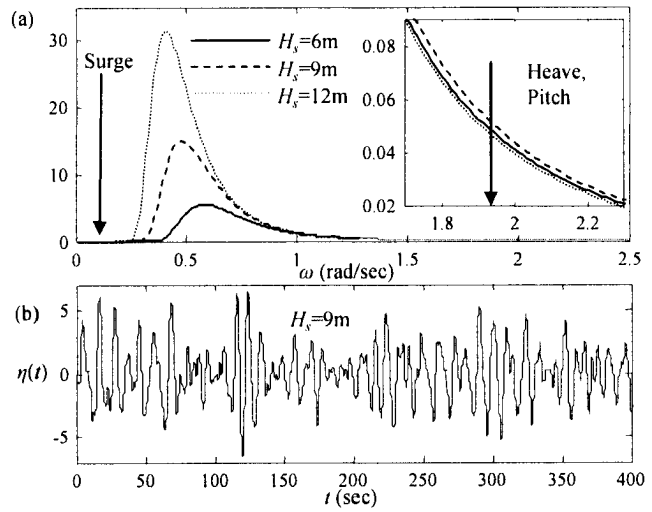

Fig.5 : (a) PM spectrum and eigenfrequensies of TLP (arrows) and (b) a sample realization of $\eta(t)$.

Controller design

The performance criteria considered for the controller design are the structural integrity of the risers, the yielding and snapping of the tendons and the comfort of the crew. The corresponding performance variables used are the maximum heave displacement, maximum and minimum dynamic stress of the tendons and the root mean square acceleration in vertical and horizontal directions at the deck of the platform. The thresholds for each one are 0.25m, 450MPa (assumed yielding stress of steel), 0 (no compressive stress allowed), 0.15g and 0.07g. The latter two quantities are adopted based on the survey by Stevens and Parson (2002). Note that under the initial pretension, the stress on the tendons is 195MPa. The controller optimization is performed under the reliability-based framework described earlier using nonlinear simulations. The time duration for each simulation run is set to T_t=10min. The number of component waves, k, is set to 60 in order to reduce the computational time needed for each simulation run. Applying SSO, the design yielded the optimal passive damper parameters: period 3.1 sec and damping ratio 0.08 (same for all dampers because of symmetry). For the active case, the design yielded optimal feedback gains (not reported due to limited space). The damper parameters for the active application were set fixed to the corresponding values from the passive case.

Performance evaluation

The evaluation of the controlled system is performed with respect to (a) reliability criteria (similar to the ones considered in the design stage) and (b) the response characteristics for 12 different sea states. These sea states ultimately represent potential future excitations. They are simulated, here, according to the model presented earlier for four different significant wave heights selections; (i) H_s=12m (ii) H_s=9m (iii) H_s=6m and (iv) H_s=3m. For each H_s three different up-crossing periods are considered, corresponding to (a) the mean value and to values that are one standard deviation (b) higher or (c) lower than the mean value. These values are calculated according to the probabilistic model presented earlier, conditioned on the selection of H_s.

The reliability is evaluated for three different cases, in terms of the minimum significant wave height considered, (i) H_s>1, (ii) H_s>4 and (iii) H_s>6. The first case corresponds to the nominal probabilistic description for the site (the one assumed in the controller design stage) but the latter two cases correspond to conditioning on moderate or significant excitation events (H_s is set higher than some threshold). The efficient Subset Simulation algorithm (Au and Beck, 2001) was used for the reliability evaluations. The results are reported in Table 2. The control application significantly increases the reliability of the platform. Implementation of active control provides a considerable margin of improvement over the passive application. These comments are true for all excitation cases. Even for significant excitation events (H_s>6m), the probability of failure of the controlled system is kept small.

Table 2. Evaluation of control implementation under reliability criteria.

Case	Estimated probability of failure		
	No control	Passive TMD	Active TMD
H_s>1m	0.038	0.0017	0.0006
H_s>4m	0.121	0.0071	0.0024
H_s>6m	0.201	0.0188	0.0093

The results for the sea states are discussed next. The simulation of the response is performed over 10 min. The response quantities reported are the ones used for evaluation of the reliability performance in the controller design stage plus the maximum pitch rotation. In Table 3 some results are reported for two cases. For both of them the significant height is equal to H_s=9m, but T_z is set (i) for the first case to its conditional mean value, T_z=9.3sec, and (ii) for the second to a value one standard deviation lower, T_z=8.5sec (this corresponds to excitation closer to resonance). aRMSv and aRMSh denote the RMS deck acceleration in the vertical and horizontal directions, respectively. Fig. 7 shows some comparative scatter diagrams of the response for all cases. Some indicative time histories are illustrated in Fig. 6.

Table 3. Evaluation of control implementation for simulated sea states.

		No control	Passive	Active
(i)H_s=9, T_z=9.3	Max(|z|)	0.35 m	0.27 m	0.23 m
	Max(|θ|)	0.0091 rad	0.0074 rad	0.0061 rad
	Max(stress)	381 MPa	327 MPa	291 MPa
	Min(stress)	-1.18 MPa	50 MPa	82 MPa
	aRMSv	0.032 g	0.019 g	0.011 g
	aRMSh	0.054 g	0.035 g	0.028g
(ii)H_s=9, T_z=8.5	Max(|z|)	0.39 m	0.31 m	0.30 m
	Max(|θ|)	0.0101 rad	0.0083 rad	0.0079 rad
	Max(stress)	404 MPa	336 MPa	312 MPa
	Min(stress)	-3.18 Mpa	47 MPa	43 MPa
	aRMSv	0.032 g	0.021 g	0.012 g
	aRMSh	0.054 g	0.039 g	0.031 g

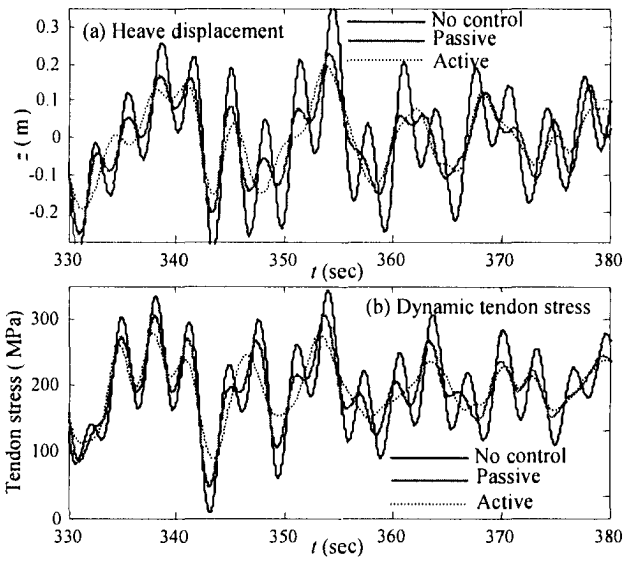

Fig.6: Time histories for heave displacement and tendon stress for simulated sea state with properties H_s=9m, T_z=10.6 sec.

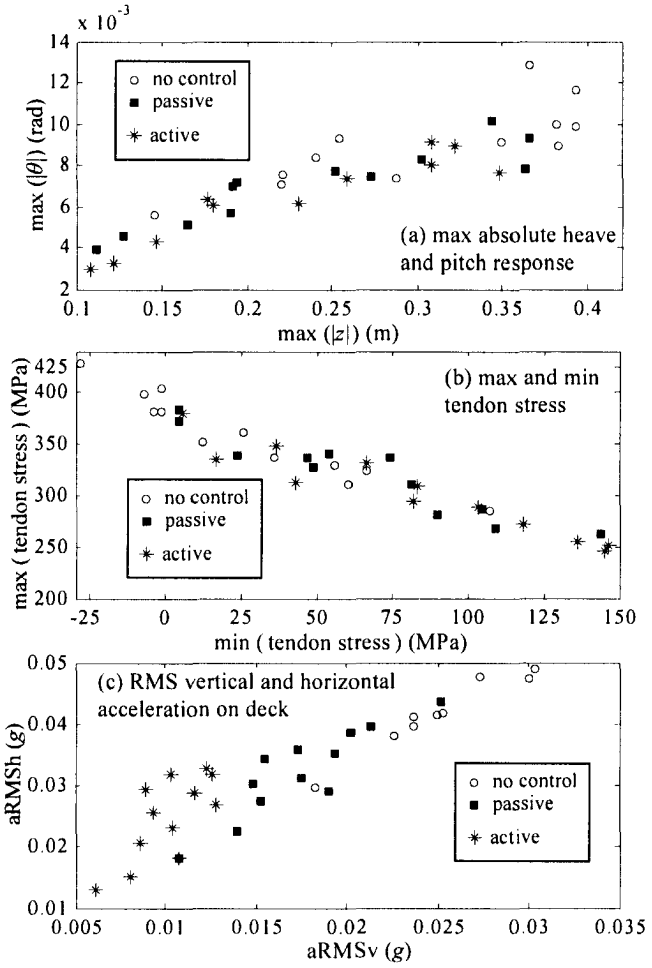

Fig.7 : Scatter diagrams of response for 12 simulated sea states.

The results further verify the effectiveness of the control application. It is important to note that the dynamic strain of the uncontrolled system in some of the excitations cases becomes negative (Fig. 7(b)). Under most quantifications of acceptable performance, i.e. even if one did not use the thresholds assumed in the controller design stage, such response may cause failure because it leads to snapping of the tendons. This unacceptable performance is eliminated in the TMD-equipped platform. This shows the effectiveness of the control application in protecting the integrity of the platform under severe weather conditions. Overall the response of the controlled system, as indicated in the scatter diagrams of Fig. 7, illustrates a significant improvement over the uncontrolled one. This holds for both the pitch and heave responses separately, as indicated in Fig. 7(a), as well as for their coupled effect, which is represented by the tendon stress in Fig. 7(b). Since the average performance is easier to regulate than the extreme one, the improvement in terms of the RMS acceleration is even greater (compare Fig. 7(c) to Fig. 7(b) or Fig. 7(a)).

Finally, a comparison between the passive and active control implementations is warranted. In terms of both the reliability evaluation (Table 2) and the simulated sea states (Table 3 and Fig. 7), the active control application provides an improvement over the passive one. For the simulated sea states, this improvement is more evident for the RMS response (Fig. 7(c)), for similar reasons as explained above. The margin of improvement over the passive control application is of course smaller when compared to the margin between the "passive control" and "no control" cases. This is expected since the passively controlled system represents a system that is considerably enhanced over the uncontrolled one. Thus further improvement of its performance is more challenging. Note, also, that the setting for the active control application assumed here incorporates many practical constraints that reduce the control effectiveness. This is apparent from the results of Table 3. Recall that case (ii) represents excitation conditions closer to resonance. This leads to operation of the actively controlled system closer to its constraints in terms of both (a) actuator saturation and (b) allowable damper displacement, and consequently to some degradation of performance (the constraints are actually violated in this case, not shown in the paper due to space limitations). This is why smaller improvement over the passive control applications appears for the extreme response quantities, when compared to case (i) of Table 3. Overall, the improvement in performance, in particular with respect to the system reliability, shows that the application of active control techniques should be considered as an attractive extension in control of Tension Leg Platforms when Tuned Mass Dampers are used. The fact that the setting considered for the active control implementation in this study takes into account most practical constraints and may be considered feasible, based on current actuator, sensor and software capabilities, further supports this conclusion.

CONCLUSIONS

A robust-to-uncertainty, nonlinear controller design for offshore structures was discussed in this paper. A methodology was illustrated that uses reliability criteria to assess the favorability of different controllers and stochastic simulation to evaluate the response of the controlled system. The controller optimization is challenging but can be efficiently performed using a powerful tool, Stochastic Subset Optimization, that has been recently developed. In this simulation-based framework, all nonlinear characteristics of the controlled system can be potentially incorporated into the system model. Also, uncertainty about the model parameters can be treated using reasonable probabilistic descriptions. Ultimately, the effectiveness of this methodology depends on the ability of the adopted model to represent (a) the structural system, and (b) future excitations. If the representation

is accurate and the uncertainty about the model parameters is quantified properly, the proposed methodology provides a powerful tool for designing the controlled system by taking into account all of its important (linear or nonlinear) characteristics and its uncertainties and this can provide significant improvement of the system performance. The only consideration for the complexity in the system description is the available computational power for efficiently performing multiple simulation analyses.

Application to a Tension Leg Platform was discussed. Implementation of both passive and active tuned mass dampers was considered for realization of the control force on the structure. The total mass of the damper was kept to a feasible level. A realistic setting was considered for the control application: actuator saturation, availability of only noisy acceleration measurements, constraints in the maximum damper displacements and time delay in the control loop were taken into account. For the active application, acceleration feedback was chosen which is easy to implement and corresponds to a reliable controller structure selection. The results illustrate significant reduction in important response quantities for both (a) the integrity of the oil risers and the tendons of the platform as well as (b) the comfort of the crew. This shows the efficiency of both the controller design methodology and the capabilities of the suggested control implementation for TLPs. The active control case illustrated improvement over the passive one, which justifies further exploration of such techniques when considering control applications to TLPs.

REFERENCES

Ahmad SK and Ahmad S (1999). "Active control of non-linearly coupled TLP response under wind and wave environments," *Computers and Structures*, No 72, pp 735-747.

Alves RM and Batista CR (1999). "Active/Passive control of heave motion for TLP type of offshore platforms," *9th International Offshore and Polar Engineering Conference*, Brest, France, Vol 1, pp 332-338.

Anderson BDO and Moore JB (2005). *Optimal filtering*. Dover publications Mineola, New York.

Angelides DC, Chen C-Y and Will SA (1982). "Dynamic response of tension leg platform," *3rd International conference on Behaviour of Off-shore Structures*, Vol 2, pp 100-120.

Au SK and Beck JL (2001). "Estimation of small failure probabilities in high dimensions by subset simulation," *Probabilistic Engineering Mechanics*, Vol 16, pp 263-277.

Chakrabarti SK (1971). "Discussion of dynamics of single point moorings in deep water. ," *Journal of Waterways, Harbour and Coastal engineering*, Vol 97, pp 558-590.

Chandrasekaran S and Jain AK (2002). "Triangular configuration tension leg platform behaviour under random sea wave loads," *Ocean Engineering*, Vol 29, pp 1895-1928.

Chu SY, Soong TT and Reinhorn AM (2006). *Active, hybrid and semi-active structural control: A design and implementation handbook*. John Wiley & Sons: Chichester, England.

Goda Y (2000). *Random seas and design of maritime structures*. World Scientific Publishing: Singapore.

Mathisen J and Bitner-Gregersen E (1990). "Joint distributions for significant wave height and wave zero up-crossing period," *Applied Ocean Research*, Vol 12, No 2, pp 93-103.

Mekha BB, Johnson CP and Roesset JM (1996). "Implications of tendon modeling on nonlinear response of TLP," *Journal of Structural Engineering*, Vol 122, No 2, pp 142-149.

Nakamura M, Kajiwara H, Koterayama W and Hyakudome T (1997). "Control system design and model experiments on thruster assisted mooring system " *7th International Offshore and Polar Engineering Conference*, Honolulu, Hawai, Vol 1, pp 641-648.

Papadimitriou C, Beck JL and Katafygiotis LS (2001). "Updating robust reliability using structural test data," *Probabilistic Engineering Mechanics*, Vol 16, pp 103-113.

Stevens SC and Parson MG (2002). "Effects of motion at sea on crew performance: a survey," *Marine Technology*, Vol 39, No 1, pp 29-47.

Suhardjo J and Kareem A (2001). "Feedback-feedforward control of offshore platforms under random waves," *Earthquake Engineering and Structural Dynamics*, Vol 30, pp 213-235.

Taflanidis AA, Scruggs JT and Beck JL (2006). "Reliability-based performance objectives and probabilistic model uncertainty in optimal structural control," *4th World Conference on Structural Control and Monitoring*, San Diego, CA, pp in press.

Taflanidis AA and Beck JL (2007). "Efficient simulation-based optimization for optimal reliability problems," *10th International Conference on Applications of Statistics and Probability in Civil Engineering*, Tokyo, Japan.

Zeng X, Liu Y, Shen X and Wu Y (2006). "Nonlinear dynamic response of tension leg platform," *16th International Offshore and Polar Engineering Conference*, San Fransisco, California, USA, pp 94-100.

APPENDIX A

The selection of the component frequencies ω_i for the representation of the random sea is addressed in this Appendix. These frequencies should be chosen so that (a) they do not constitute harmonics with each other, and (b) describe adequately the whole frequency range of significant excitation. The procedure described in Chandrasekaran and Jain (2002) is adopted here. Let $[\omega_{\min}, \omega_{\max}]$ denote the frequency range that is important and consider the division into k-1 sub-ranges by:

$$\omega_1^* = \frac{\omega_{\max} - \omega_{\min}}{k-1}, \quad \omega_i^* = \omega_1^* \left(\frac{\omega_{\max}}{\omega_1^*} \right)^{\frac{i-1}{k-2}} \tag{21}$$

then select at random (following a uniform distribution), the dividing frequencies $\omega_1^*, \ldots, \omega_{k-1}^*$ in each of these sub-ranges and set $\omega_0^* = \omega_{\min}$ and $\omega_k^* = \omega_{\max}$. This new sequence $\{\omega^*\}$ defines finally the sub-ranges for the selection of ω_i :

$$\omega_i = \frac{1}{2}\left(\omega_i^* + \omega_{i-1}^*\right), \quad \Delta\omega_i = \omega_i^* - \omega_{i-1}^* \tag{22}$$

This methodology leads to selection of uncorrelated frequencies ω_i. Also, it efficiently describes, in a stochastic simulation setting, the energy content in the whole range of the spectrum that is considered important for the response, even for small number of component waves, k. This is established by the randomness in the selection of the frequencies ω_i^* in the different simulation runs. Note that alternative methods have been suggested for cases where k is large (for example, partitioning the spectrum into equal areas without employing any randomness, as discussed in Goda (2000). In this application, the above methodology was preferred because k was selected "relatively" small.